J. Membrane Biol. 204, 11–21 (2005)
DOI: 10.1007/s00232-005-0742-y

The Journal of
Membrane
Biology

$P2X_7$ Receptor Stimulation of Membrane Internalization in a Thyrocyte Cell Line

M.Y. Kochukov, A.K. Ritchie
Department of Physiology and Biophysics, University of Texas Medical Branch, 301 University Boulevard, Galveston, TX 77555-0641, USA

Received: 25 October 2004/Revised: 10 March 2005

Abstract. Using fluorescent membrane markers, we have previously shown that extracellular ATP stimulates both exocytosis and membrane internalization in the Fisher rat thyroid cell line FRTL. In this study, we examine the actions of ATP using whole-cell recording conditions that favor stimulation of membrane internalization. ATP stimulation of the $P2X_7$ receptor activated a reversible, Ca^{2+}-permeable, cation conductance that slowly increased in size without changes in ion selectivity. ATP also induced a delayed irreversible decrease in cell capacitance (C_m) that was equivalent to an 8% decrease in membrane surface area. Addition of guanosine 5′-0-2-thiodiphosphate to the pipette solution inhibited the ATP-induced decrease in C_m without affecting channel activation. The effects of ATP on membrane conductance were mimicked by 2′,3′-O-(4-benzoylbenzoyl)-ATP, but not by UTP, adenosine, or 2-methylthio-ATP, and were inhibited by pyridoxal phosphate-6-azophenyl-2′4′-disulfonic acid, adenosine 5′-triphosphate-2′3′-dialdehyde, and Cu^{2+}. The capacitance decrease persisted in Na^+-, Ca^{2+}- and Cl^--free external saline or with Ca^{2+}-free pipette solution. It is concluded that ATP activation of the inotropic $P2X_7$ receptor stimulates membrane internalization by a mechanism that involves intracellular GTP, but does not require internal Ca^{2+} or influx of Na^+ or Ca^{2+} through the receptor-gated channel.

Key words: P2X7 receptor — ATP — Endocytosis — Thyroid — Patch clamp

Introduction

The function of thyroid epithelial cells is regulated by TSH via G-protein receptors that are coupled to adenylyl cyclase and phospholipase C (Cerbo & Corda, 1999). Extracellular ATP, acting in cooperation with other endocrine and paracrine factors, is also a regulator of thyroidal function. In the Fisher rat thyroid cell line FRTL-5 (Smallridge & Gist, 1994; Ekokoski et al., 2000, 2001), and in primary thyrocyte cultures from a variety of species (Golstein et al., 1992; Lejeune et al., 1996; Bourke et al., 2001; Schofl et al., 2002), ATP stimulates Ca^{2+} mobilization, mitogenesis, production of H_2O_2, thyroglobulin secretion, efflux of iodide and chloride, and inhibition of forskolin-stimulated Na^+ absorption. These effects are mimicked by UTP and primarily occur via G-protein-coupled P2Y purinoceptors that activate PLC and PLA_2. The P2Y receptor subtypes that have been detected in FRTL-5 cells by RT-PCR include $P2Y_2$, $P2Y_4$, and $P2Y_6$ (Ekokoski et al., 2001). Members of the ionotropic P2X receptor family are also present. $P2X_3$, $P2X_4$ and $P2X_5$ subtypes have been detected in the thyroid gland by immunohistochemistry (Glass & Burnstock, 2001) and in FRTL-5 by RT-PCR (Ekokoski et al., 2001). Recently, we also found $P2X_7$ receptor immunoreactivity and $P2X_7$ receptor-gated cation currents in FRTL cells (Kochukov & Ritchie, 2004), the parent cell line of FRTL-5. $P2X_7$ receptors are prominent in immune cells (Gu et al., 2000; Solle et al., 2001) where they induce apoptosis and secretion of inflammatory mediators. $P2X_7$ receptors are also highly expressed in epithelial cells (Bradford & Soltoff, 2002), although their role in epithelial function is uncertain.

FM1-43, a membrane-impermeant dye that fluoresces in lipid environment, is a widely used marker for the study of plasma membrane trafficking. Using the dye, we reported that $P2X_7$ receptor activation stimulated both exo- and endocytosis in FRTL cells (Kochukov & Ritchie, 2004). However, FM1-43 is not an ideal marker of plasma membrane trafficking, as the dye undergoes a large increase in fluorescence intensity following phospholipid scrambling, an early

Correspondence to: A.K.Ritchie; email: aritchie@utmb.edu

Table 1. Ionic composition of bath solution (in mM)

	Na^+	K^+	Ca^{2+}	Mg^{2+}	NMDG	EGTA	Cl^-	Gluconate
A Standard	150	5.5	2	2	0	0	158	0
B Na-free	0	5.5	2	2	156	0	164	0
C Ca-free	155	5.5	0	2	0	2	153	0
D Na/K/Mg-free	0	0	2	0	163	0	162	0
E Na/K/Mg-free	0	0	5	0	158	0	163	0
F NaK/Mg-free	0	0	10	0	150	0	165	0
G 100 Ca	0	0	100	0	5	0	200	0
H Cl-free	155	5.5	2	2	0	0	0	163

event in apoptosis (Zweifach, 2000). The $P2X_7$ receptor is known to induce apoptosis in many cell types, which may partly account for the profound ATP-induced increases in FM1-43 fluorescence intensity that we encountered in our earlier study. In this report, we use voltage-clamp measurements of whole-cell capacitance to monitor effects of ATP on plasma membrane surface area. We also examined the Ca^{2+} permeability of the ATP-gated cation channel. Our results show that ATP stimulates exocytosis and a decrease in plasma membrane surface area that is likely due to membrane internalization. Although the ATP-gated cation-selective channel is permeable to Ca^{2+}, the $P2X_7$ receptor-mediated decrease in cell surface area occurs independently of extra- or intracellular Ca^{2+} by a mechanism that involves internal GTP.

Materials and Methods

Cell Culture

Measurements were performed on the FRTL Fisher rat thyroid cell line (Ambesi-Impiombato, Parks, & Coon, 1980) that was obtained from the American Type Culture Collection (Rockeville, MD). The cells were grown in Coon's F12 medium containing 0.5% calf serum, 10 μg/ml insulin, 10 nM hydrocortisone, 5 μg/ml transferrin, 10 ng/ml glycyl-L-histidyl-L-lysine acetate, 10 ng/ml somatostatin, and 10 mU/ml TSH and maintained in a humidified 5% CO_2 incubator at 37°C. For the electrophysiological experiments, the cells were used 1–2 days after plating on glass cover slips.

Capacitance and Current Measurements

An EPC7 patch clamp amplifier (Adams List, Great Neck, NY), the ruptured-patch technique of whole-cell recording (Hamill et al., 1981), Pulse-HEKA software and the ITC18 computer interface (Instrutech, Port Washington, NY) were used for data acquisition and analyses. The recording pipettes were pulled from 7052 glass (Garner Glass, Claremont, CA) and the tips were coated with Sylgard. The bath was grounded with a Ag/AgCl pellet and a 1 M KC1 agar bridge. Bath temperature was maintained by heating a 100 μ1 chamber to 36 °C with a feedback regulator (Warner Instruments, Hamden, CT). A small coverslip chip containing cells was placed in the chamber and continuously superfused with prewarmed solution by gravity flow at a rate of 0.5 ml/min. Upon changing the solution composition, chamber equilibration occurred within 2.5 min including about 60 s of dead space. The timing of ATP administration that is illustrated in the figures includes the dead space time. In experiments requiring rapid solution changes, ATP was applied to the cell from a large bore pipette placed ~340 μm from the cell while the chamber was continuously perfused with bath solution. In some experiments, we determined the time course of changes in current amplitudes while simultaneously monitoring the reversal potential (V_{rev}) of the ATP-activated current. The voltage steps applied for measurements of the *I-V* relationships required 6 s to complete and were executed 10 times per min. The continuous record of the current at the holding potential was obtained from current measurements made during the interval between voltage steps (2/s). When the bath solution contained NMDG or gluconate as replacements for Na^+ or Cl^-, we applied a correction to the clamped potential for the differences in liquid junction potential between the recording pipette and the bath solution.

Continuous measurements of whole-cell capacitance (C_m) were performed using the Lindau-Neher method (Lindau & Neher, 1988) and was implemented via the sine+dc lock-in feature of PulseHEKA. For measurements of C_m, the cell was clamped with a 1 kHz, 40 mV peak-to-peak, sine wave superimposed on a –80 mV holding potential. Acquired data were filtered at 10 kHz. The instrumental phase angle was adjusted to zero at the beginning of each recording period by connecting the input stage to ground via a 10 MΩ resistor. Cell membrane conductance in parallel with the seal resistance is reported as G_m and was determined from assessment of the holding current. The series access resistance (G_s) and cell capacitance were determined, respectively, from the in-phase and the 90° phase-shifted components of whole-cell admittance.

The mean C_m of 40 ± 4 pF (n = 14) was measured from cells with a mean diameter of 29 ± 2 μm. Assuming a spherically shaped cell, we calculated a specific membrane capacitance of 1.5 μF/cm^2. This value is larger than expected for a lipid bilayer (1 μF/cm^2) suggesting infolding of the plasma membrane. In the absence of stimuli, spontaneous changes in C_m were small (200–400 fF). Cells with unstable G_m or G_s were excluded from analysis since large changes in these parameters can affect the measurement of C_m.

Solutions

The pipette solution contained (in mM): 25 CsCl, 65 Cs_2SO_4, 2 EGTA, 0.6 $CaCl_2$ (100 nM free Ca^{2+} at 36°C), 3 $MgCl_2$, 10 NaCl, 10 glucose, 60 sucrose, and 10 HEPES. The pH was adjusted to 7.04 (at 36 °C) with CsOH (8 mM). The measured osmolality (Wescor 5500 vapor pressure osmometer, Logan, UT) was 305 mOsm. Ca^{2+}-free pipette solution contained 0 added Ca^{2+} and 4 mM BAPTA instead of EGTA. The bath saline consisted of the ions listed in Table 1 plus (in mM) 5 glucose, 10 HEPES, and sucrose (~40 mM) as needed to obtain a final osmolality of 335 mOsm. The pH was adjusted to 7.4 (at 36 °C) with NaOH or NMDG. Stock solutions of 50 mM ATP or 5 mM UTP were prepared in nominally

Ca^{2+}-free bath solution, then subsequently adjusted to pH 7.4 and ~335 mOsm. Na^+-free stock solutions of ATP were prepared with N-methyl-D-glucamine (NMDG) as the major cation. All experiments were performed at 35–36 °C. The program Webmaxlite v1.15, courtesy of C. Patton at www.stanford.edu/~cpatton/maxc.html, was used to calculate the concentrations of free Ca^{2+} and ATP^{4-}.

Analyses

The relative permeabilities of the ATP activated channel to Ca^{2+} (P_{Ca}), Cs^+ (P_{Cs}) and NMDG (P_{NMDG}) were estimated from the following rearrangement of the Goldman-Hodgkin-Katz equation (Korngreen et al., 1998; Lewis, 1979):

$$V_{rev}=\frac{RT}{F}\ln\left\{\frac{1}{2}\left[\frac{P_{NMDG}\gamma_{NMDG}[NMDG]_o}{P_{Cs}\quad\gamma_{Cs}\quad[Cs]_i}-1+\left[\left[1+\frac{P_{NMDG}\gamma_{NMDG}[NMDG]_o}{P_{Cs}\quad\gamma_{Cs}\quad[Cs]_i}\right]^2+16\frac{P_{Ca}\gamma_{Ca}[Ca]_o}{P_{Cs}\gamma_{Cs}\,[Cs]_i}\right]^{1\backslash 2}\right]\right\} \quad (1)$$

At 36°C, the constant RT/F equals 26.7 mV. The equation is valid when the extracellular solution contains a permeant monovalent cation and divalent cation and the intracellular solution contains one permeant cation. We considered the permeability of intracellular Na^+ (10 mM) to be similar to Cs^+ and used their combined concentration for total $[Cs^+]_i$. The intracellular free $[Ca^{2+}]$ of 100 nM was assumed to be negligible. We used the activity coefficients (γ) reported for 25°C, as they are within 2% of the values at 35°C. A γ of 0.75 was used for both Cs^+ (Robinson & Stokes, 1959) and NMDG (Lindenbaum & Boyd, 1964). For γ_{Ca} we used 0.28, which is the square of the mean activity coefficient reported for CaCl ($\gamma_{\pm}$ = 0.53) in mixed solutions of 0.16 ionic strength (Butler, 1968).

Results are reported as mean ± SEM. Statistical significance ($P < 0.05$) was determined using Kruskal-Wallis rank sum statistics and Dunn's multiple comparison test (Sigma Stat 2.0, SPSS Inc, Chicago, IL). The same set of control responses to ATP was used in Figures 6, 7, and 8. Curve fitting and regression analysis were done with SigmaPlot 8.0 (SPSS Inc., Chicago, IL).

Chemicals

Hydrocortisone, bovine apo-transferrin, bovine insulin, somatostatin, glycyl-L-histidyl-L-lysine acetate, calf serum from donor herd, ATP-sodium salt, adenosine, guanosine 5′-0-2-thiodiphosphate trilithium salt (GDPβS), pyridoxal phosphate-6-azophenyl-2′4′-disulfonic acid tetrasodium salt (PPADS), adenosine 5′triphosphate-2′3′-dialdehyde sodium salt (oxoATP), 2′,3′-O-(4-benzoylbenzoyl)-ATP trimethylammonium salt (BzATP), and ARL 67156 were obtained from Sigma Chemical (St. Louis, MO). UTP-sodium salt and 2-methylthio-ATP tetra sodium salt (2MeSATP) were from CalBiochem (La Jolla, CA), R(-)N6-(2-phenylisopropyl) adenosine (PIA) was from Research Biochemicals International (Natick, MA) and TSH, from Dr. A. F. Partlow (National Hormone and Peptide Program, Torrance, CA).

Results

Characteristics of the ATP-gated Current

Currents were measured under whole-cell voltage clamp in response to prolonged (5 min) administration of 500 μM ATP from a large-bore pipette. In standard saline (Solution A, Table 1), ATP rapidly evoked an inward current with a long-lasting plateau and rapid reversal on washout of ATP (Fig. 1*A*). On second exposure to the same dose, the current slowly grew in amplitude, and the third exposure evoked a much larger initial current that also grew in amplitude. Typically, the initial current on repeat application was equal to the amplitude at the end of the previous application of ATP, indicating a long-lasting priming action of ATP (Korngreen et al., 1998). To determine if the increase in amplitude was correlated with a change in ion selectivity, reversal potentials were determined from current amplitudes measured at different voltages in the absence and presence of ATP. The I-Vs measured during the second exposure to ATP are shown in Fig. 1*B*. Although the current amplitudes increased with each successive *I-V* measurement, *Vrev* (the zero-current potential) remained constant. The reversal potentials are plotted underneath the current trace in Fig. 1*A*. It can be seen that the growth in current amplitude is not accompanied by a change in ion selectivity. Hence, the current growth is likely due to the activation of additional ATP-gated channels, although we cannot exclude slow activation of a different kind of channel with the same ion selectivity. V_{rev} in this cell was +6 mV, consistent with our previous observation (Kochukov & Ritchie, 2004) that ATP stimulation of the $P2X_7$ receptor in FRTL cells gates a cation-selective channel that is permeable to Na^+ and Cs^+.

To determine the Ca^{2+} permeability of the ATP-gated channel, we measured the reversal potential of the ATP-activated currents (Fig. 2*A*) in solutions containing different concentrations of Ca^{2+} and the organic cation NMDG, but no Na^+, K^+ or Mg^{2+} (Solutions D, E, and F in Table 1). In solutions containing NMDG and 2 mM Ca^{2+}, V_{rev} was −51.2 ± 1.6 mV (n = 5), consistent with low permeability to $NMDG^+$ (Fig. 2*B*). The reversal potential shifted to the right as Ca^{2+} was increased up to 10 mM. From the fit of the data to equation (1), P_{Ca}/P_{Cs} was estimated to be 1.34 and P_{NMDG}/P_{CS} was 0.11 (Fig. 2*C*). In 100 mM Ca^{2+} (Solution G, Table 1), ATP failed to evoke currents. This is largely due to interference with receptor activation via Ca^{2+} chelation of ATP^{4-} (Korngreen et al., 1998), although an allosteric effect on the receptor's affinity for ATP (Virginio, North, & Surprenant, 1998) or open-channel block (Nakazawa & Hess, 1993) may also be involved.

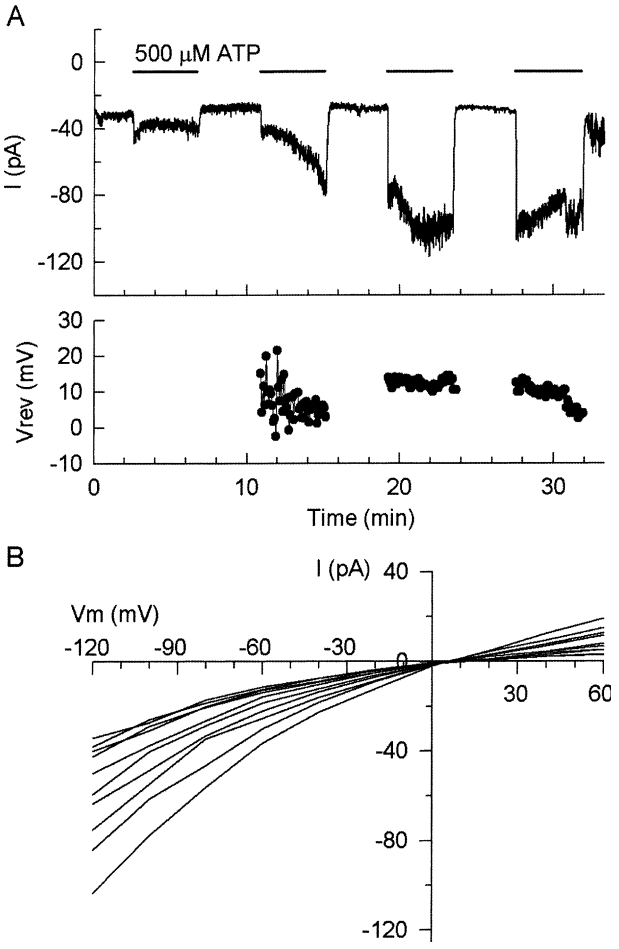

Fig. 1. Activation of ionic current by extracellular ATP. (*A*) Whole-cell currents were monitored at the −80 mV holding potential and ATP (500 μM) was applied to the cell from a large-bore pipette at the times indicated by the horizontal bars. At 10 s intervals, *I-V* plots were constructed from currents measured during 200 ms voltage steps from 120 to +60 mV in 20 mV increments. The continuous current record shown for the −80 mV holding potential was constructed from currents recorded during the interpulse intervals. The reversal potentials determined from the *I-V* relationships are plotted below the current trace. (*B*) The *I-V* plots obtained during the second application of ATP represent the currents measured in the presence of ATP after subtraction of the control currents measured at each voltage prior to the application of ATP. For clarity of presentation, each *I-V* curve represents the average of 5 consecutive *I-V* relationships. The current amplitudes increased with time, but the reversal potential remained constant. The *I-V* relationship during the 1st application of ATP was difficult to perform due to the small size of the current and contamination from a voltage-gated Ca^{2+} current that washed out during the first 10 min of recording.

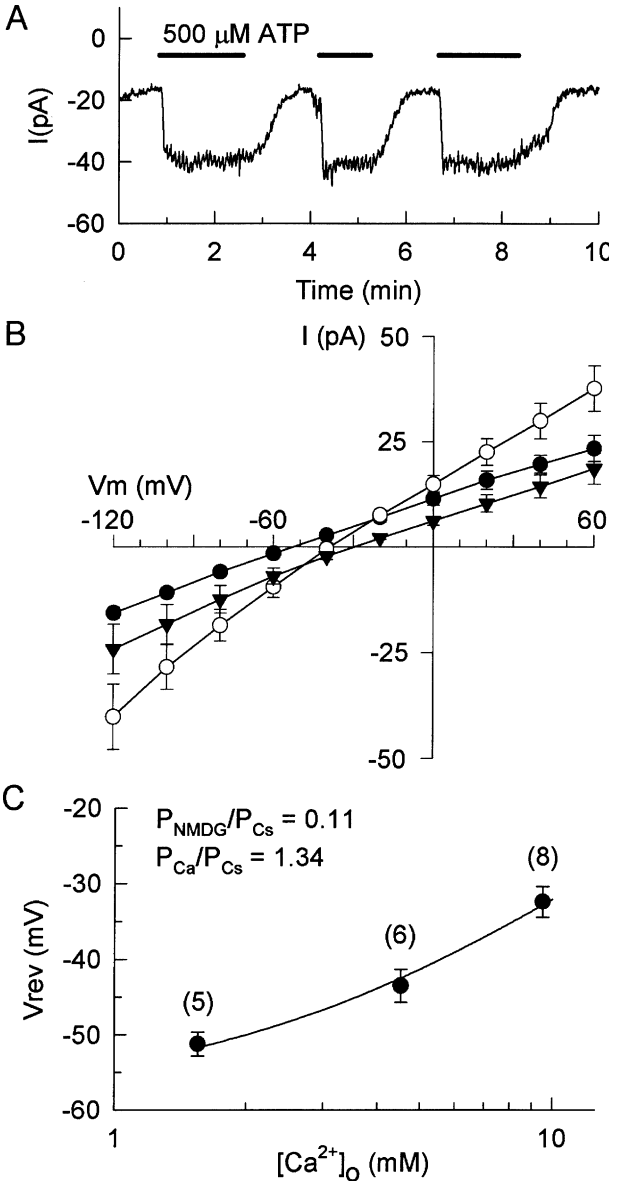

Fig. 2. Ca^{2+} permeability of the ATP-activated channel. (*A*) Currents activated by multiple applications of 500 μM ATP from a large-bore pipette were recorded at −80 mV in Na^+, K^+, and Mg^{2+} -free saline with $NMDG^+$ and Ca^{2+} as the major cations. In this example, the first application of ATP was performed in 10 mM external Ca^{2+} and the next two in 5 mM Ca^{2+}. (*B*) *I-V* relationships of the ATP-activated current ($I_{ATP}-I_{control}$) were measured in 2 (*filled circles*, $n = 5$), 5 (*empty circles*, $n = 6$), and 10 (*inverted triangles*, $n = 8$) mM external Ca^{2+}. (*C*) The mean reversal potentials ± SEM (number of cells in parentheses) are plotted as a function of the log of the external free $[Ca^{2+}]$, after correction (Maxlite software) for Ca^{2+} complexed with ATP. Relative cation permeabilities, P_{NMDG}/P_{Cs} and P_{Ca}/P_{Cs}, were obtained from the best fit (indicated by the curved line; R^2, the coefficient of determination, = 0.7261) of the data to Equation (1).

In standard saline, 500 μM ATP evokes current, but 200 μM ATP is ineffective. The low affinity for ATP is not due to the presence of ecto-ATPases, as we did not observe any changes in ATP sensitivity after pretreatment with the ecto-ATPase inhibitor ARL 67156 (100 μM). The low affinity of the receptor for total ATP in solutions containing divalent cations is a distinguishing feature of the $P2X_7$ receptor, as the active ligand is the uncomplexed ATP^{4-}. Removal of extracellular Cl^-, which has no effect on V_{rev} (Kochukov & Ritchie, 2004), has a dramatic effect on the

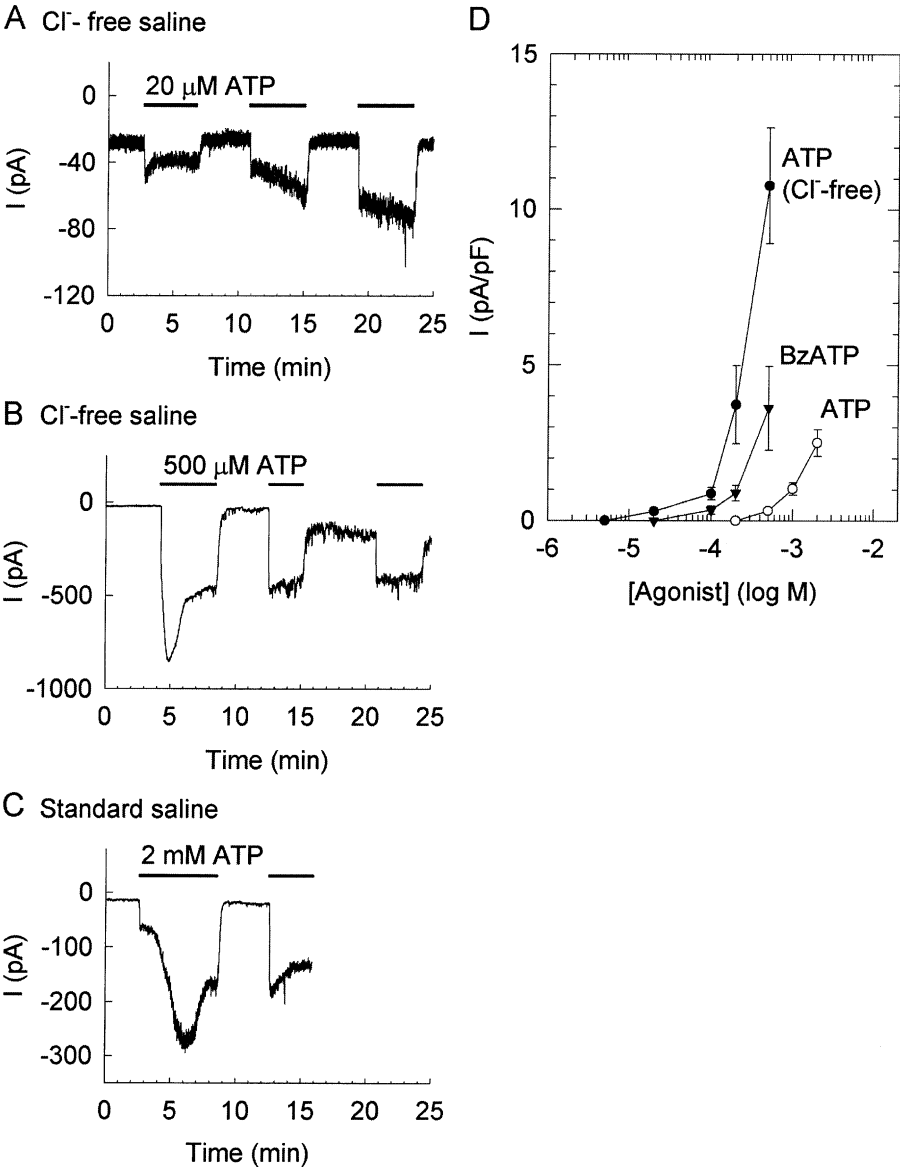

Fig. 3. Agonist-response relationships. Agonists were applied from a large-bore pipette and currents were recorded at −80 mV. *A* and *B* represent currents activated by 20 and 500 μM, ATP respectively, in Cl^- -free external saline with gluconate as the replacement anion and currents in *C* were evoked by 2 mM ATP in standard external saline. (*D*) The instantaneous current amplitudes in response to the first application of ATP ($n \geq 3$) in standard saline, ATP in Cl^--free saline ($n = 2$ for 100 μM ATP and ≥ 4 for the remaining doses), or BzATP in standard saline ($n = 4$) were normalized to cell C_m and plotted as a function of the external ATP or BzATP concentrations.

potency of ATP. As seen in Fig. 3, 20 μM ATP in Cl^--free saline (Solution H, Table 1) has an amplitude and time course that is similar to that evoked by 500 μM ATP in standard saline (Fig. 1*A*). Likewise, the current evoked by 500 μM ATP in Cl^--free saline activates a current with larger initial amplitude, faster growth, slow desensitization, and incomplete deactivation that is more typical of the current evoked by 2 mM ATP in standard saline. Partial dose-response curves, constructed from the rapid initial current amplitudes in response to the first application of ATP, show that much lower concentrations of ATP are effective in Cl^--free solutions (Fig. 3*D*). The graph also shows that BzATP, a synthetic agonist of most P2X receptors, activates current at lower concentrations than ATP in standard saline. The apparent higher potencies of BzATP and ATP in Cl^-free solution in comparison to ATP in standard saline are characteristic features of $P2X_7$ receptors (Michel, Chessell, & Humphrey, 1999).

Effects of ATP on C_M and G_M

Whole-cell lock-in phase measurements of C_m were performed to study the effects of $P2X_7$ receptor activation on cell surface area, with simultaneous

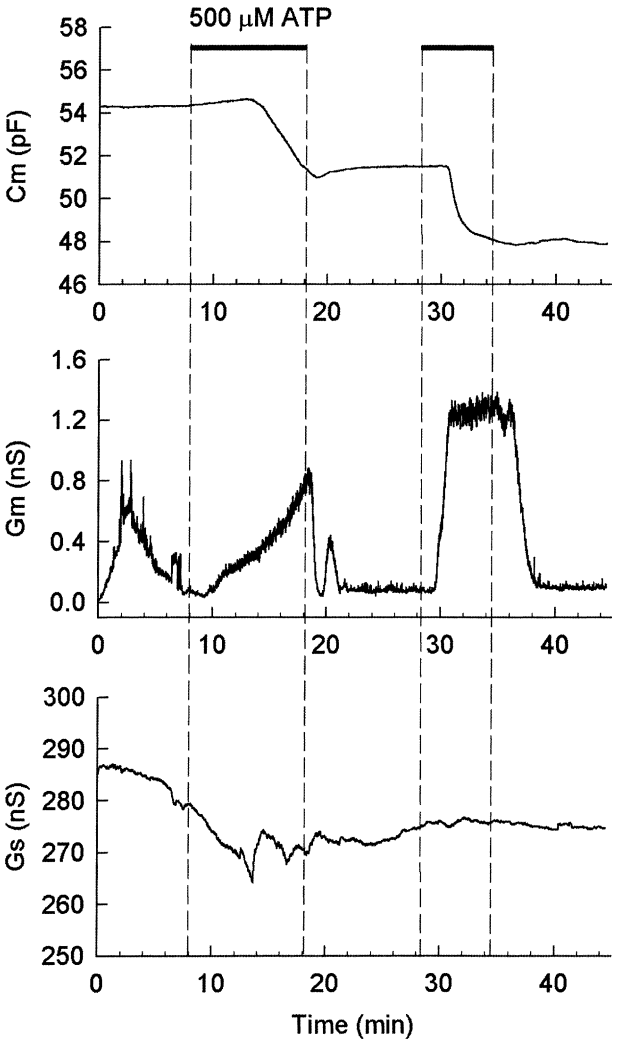

Fig. 4. Effects of extracellular ATP on C_m, G_m and G_s. The cell was clamped with a 1 kHz sine wave superimposed on the −80 mV DC holding potential. The solution perfusing the chamber was switched from standard saline to saline containing 500 μM ATP during the times indicated by the bars. ATP, applied twice, irreversibly decreased C_m, reversibly increased G_m, and had no effect on G_s. The initial spontaneous transient increase in G_m was observed in most cells and was likely related to cell dialysis by the pipette.

assessment of changes in membrane conductance. In nearly all cells, G_m showed an initial spontaneous transient increase that was likely related to washout of cytosolic constituents and equilibration with pipette solution (Fig. 4, *middle trace*). An 8–10 min application of 500 μM ATP by bath perfusion induced a slowly rising increase in G_m that rapidly reversed on washout of ATP. Upon reapplication of ATP to the same cell, the increase in G_m was faster and larger.

The changes in G_m reflect the ATP-induced ionic currents shown in Fig. 1, although with a different time course that is probably due to the slower rate of equilibration when ATP is applied by bath perfusion and the much longer duration of ATP application.

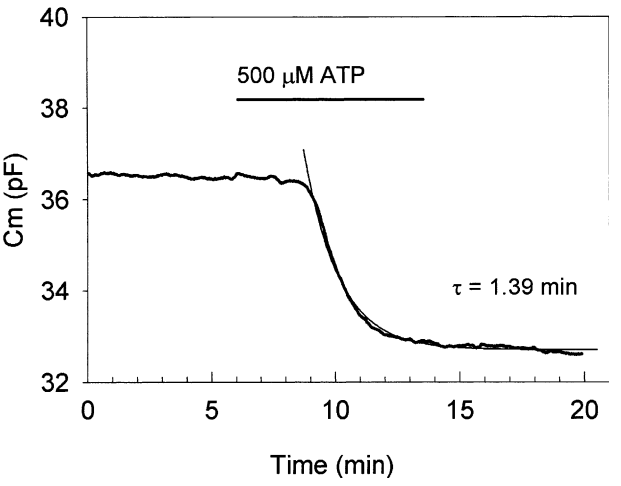

Fig. 5. The time course of the ATP-induced decrease in cell capacitance. In cells where ATP was applied by bath perfusion for > 5 min, the time course of the capacitance response was fit to an exponential decay ($y = A_0 + A_1\exp(-t/\tau)$, where A_0 is the C_m at $t = \infty$ and A_1 is the change in C_m between $t = 0$ and $t = \infty$). The C_m recording is shown with a thick line and the exponential fit is overlayed in thin line ($\tau = 1.39$ min and $R^2 = 0.9916$).

ATP also induced a delayed decrease in C_m to a new level, although occasionally, a tiny portion of the decrease in C_m was reversible (Fig. 4, *top trace*). The second application of ATP induced a further irreversible decrease in C_m of similar magnitude. The bottom trace shows negligible changes in pipette access conductance (G_s). The values for basal G_m and G_s correspond to resistances of ~10 GΩ and 3.6 MΩ, respectively. The absence of temporal overlap in the three simultaneously determined parameters shows that the changes in C_m are not due to technical interference caused by changes in G_m or G_s. Lack of interference by changes in G_m is not surprising as the ATP-induced increases in membrane conductance are small. On the infrequent occasions when changes in C_m occurred in temporal concert with changes in G_m or G_s, the cell was excluded from analysis. When performed at room temperature instead of 36 °C, ATP continued to evoke changes in G_m, but failed to affect C_m.

The onset of the ATP-evoked decrease in C_m was delayed by 79 ± 13 s after the beginning of the increase in G_m. When the duration of ATP application was long enough for C_m to reach a new steady-state level, the time course of the decrease in C_m was exponential (Fig. 5) and occurred with a mean time constant of 2.7 ± 0.5 min ($n = 10$ cells). The mean decrease in C_m (Fig. 6*C*), measured after 4 min in 500 μM ATP, was 3.26 ± 0.38 pF ($n = 15$ cells). This was equivalent to an 8.4 ± 0.8% decrease in cell surface area. A decrease in surface area could be caused by stimulation of membrane internalization, plasma membrane vesicle shedding, inhibition of

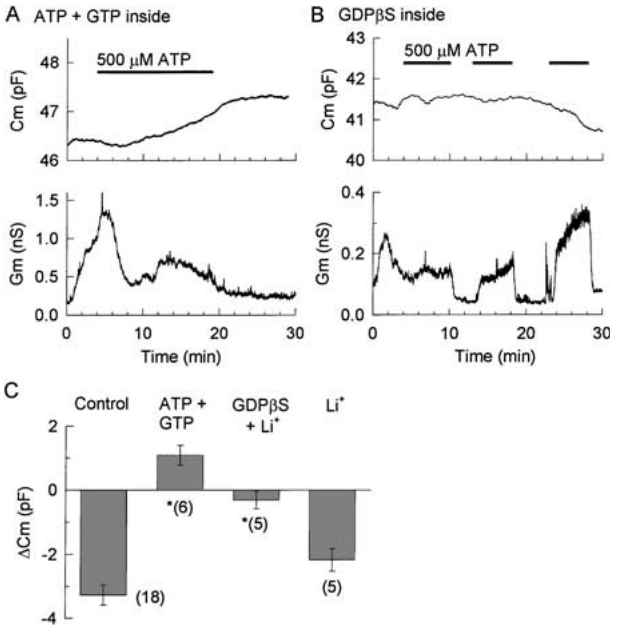

Fig. 6. Effects of intracellular ATP and GTP on the ATP-evoked changes in C_m and G_m. (*A*) Records of cell capacitance and G_m with 5 mM ATP and 10 μM GTP added to the standard pipette solution. Under these conditions, extracellular ATP produced a small net increase in C_m. (*B*) Inclusion of 2 mM GDP*β*S in the standard pipette solution blocked the capacitance, but not the conductance, change in response to extracellular ATP (500 μM). (*C*) Bar graph of the mean ATP (500 μM)-induced capacitance change in standard pipette solution (*control*) or in pipette solution also containing 5 mM ATP + 10 μM GTP, 2 mM GDP*β*S (trilithium salt) or 6 mM LiCl. The asterisk indicates significant differences from the control response. Agonists were applied by bath perfusion.

constitutive exocytosis, or a combination of events with overall net decrease in surface area.

Dependence on Intracellular ATP and GTP

The experiments shown in Figs. 4 and 5 were performed with standard pipette solution containing no added ATP or GTP. In contrast to the pronounced ATP-induced decrease in C_m observed with standard pipette solution, when 5 mM ATP and 10 μM GTP were included in the pipette solution (Fig. 6*A*), extracellular ATP evoked an increase in C_m of 1.09 ± 0.31 pF ($n = 6$). This was equivalent to a net increase in cell surface area of 3.1 ± 1.2 %. Thus, when cytoplasmic ATP and/or GTP are plentiful, extracellular ATP may stimulate exocytosis to an extent that masks the membrane internalization/shedding.

Addition of 2 mM GDP*β*S to the pipette solution, which competitively interferes with reactions that require GTP, nearly abolished the ATP-induced decrease in C_m, but not the increase in G_m (Fig. 6*B*). The effect of GDP*β*S was not due to the Li^+ salt of GDP*β*S, as the C_m response persisted when 6 mM LiCl was included in the pipette solution (Fig. 6*C*). Thus, internal GTP is essential for the ATP-induced decrease in C_m and it is not necessary for the evoked increase in membrane conductance. As GTP was not added to the pipette solution, we presume that endogenous levels of GTP that were resistant to washout supported the purinoceptor-induced decrease in C_m. The remainder of the electrophysiological experiments described in this study focus on the ATP-induced decrease in C_m (ΔC_m) and were performed with standard pipette solution containing no ATP or GTP.

Pharmacology of the ATP-Evoked Decrease in Capacitance

Different pharmacological agents were applied to study specificity of the ATP-induced decrease in cell surface area (Fig. 7). UTP (500 μM), an agonist that activates the P2Y receptors in these cells, but is a poor agonist of P2X receptors, did not evoke changes in G_m (*not shown*) or C_m. Two adenosine receptor (P1 receptor) agonists, adenosine and R-PIA, also failed to induce changes in C_m (or G_m). The P2 receptor agonist BzATP mimicked the effect of ATP on C_m, while the agonist 2MeSATP (500 μM) had a very weak effect. The ATP-induced changes in C_m were inhibited by 100 μM PPADS and 50 μM Cu^{2+}. Oxo ATP (200 μM), which was present during a 2 h pre-incubation but not during the measurement, irreversibly inhibited the response to ATP. The pharmacological profile is consistent with our previous study (Kochukov & Ritchie, 2004) and indicates mediation by the $P2X_7$ receptor.

Effects of Ion Substitutions on the Capacitance Response

Different ion substitutions in the pipette or bath solution were made to determine ion dependence of the $P2X_7$ receptor-induced decrease in C_m (Fig. 8). The decreases in C_m were not significantly different from the control responses after replacement of external Na^+ with NMDG (Solution B, Table 1), replacement of external Cl^- with gluconate (Solution H) or removal of extracellular Ca^{2+}, with addition of 2 mM EGTA (Solution C). The response also persisted when intracellular Ca^{2+} was buffered to near 0 by including the fast acting Ca^{2+} chelator BAPTA (4 mM) in the Ca^{2+} free pipette solution.

Discussion

The ion selectivity of the ATP-gated $P2X_7$ receptor channel and the role of cation flux in mediation of $P2X_7$ receptor stimulation of membrane internalization were studied. We used whole-cell patch-clamp

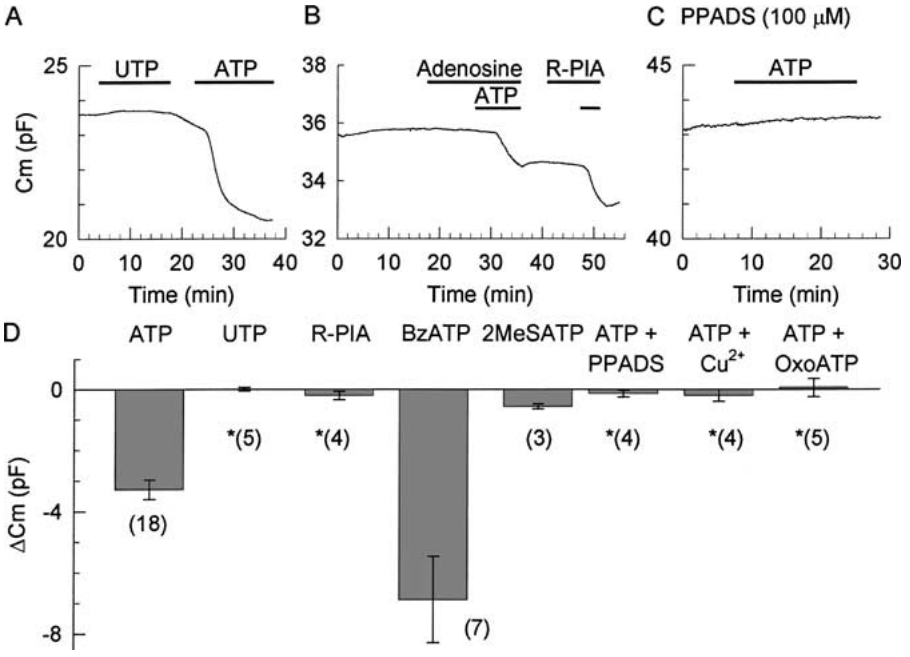

Fig. 7. Pharmacological specificity of the capacitance response. The agonists UTP (*A*), adenosine, or R-PIA (*B*) failed to evoke capacitance responses, while application of ATP (500 μM) to the same cells decreased C_m. The presence of PPADS, a purinergic receptor antagonist, blocked the effects of 500 μM ATP on C_m (*C*). The effects of agonists and antagonists on C_m are summarized in (*D*). All agonists were applied by bath perfusion and were present at a concentration of 500 μM. The antagonists PPADS (100 μM) and Cu^{2+} (50 μM) were applied just prior to and during the addition of ATP. OxoATP (200 μM) was present during a 2 h preincubation at 37°C in Coon's F12 medium and washed out before application of ATP in standard saline (without OxoATP). The numbers of cells tested are indicated in parentheses and the asterisk indicates significant differences from the response to ATP alone.

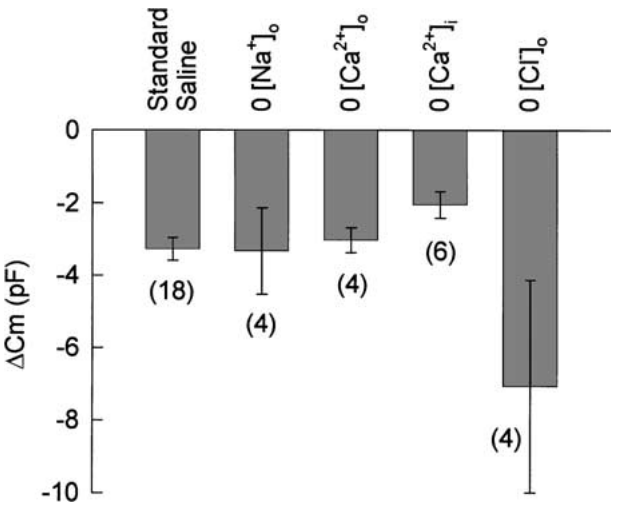

Fig. 8. Effect of Na^+, Ca^{2+}, and Cl^- on ΔC_m. The C_m response to 500 μM ATP applied by bath perfusion was determined in standard external solution and in Na^+-free (replaced by NMDG), Ca^{2+}-free (0 added Ca^{2+} + 2 mM EGTA), or Cl^--free (replaced with gluconate) external solution. The experiments with 0 internal Ca^{2+} (pipette solution with 0 added Ca^{2+} plus 4 mM BAPTA) were conducted in standard external solution. The numbers of cells are indicated in parentheses. There were no significant differences between the groups.

recording of membrane capacitance, which directly measures changes in cell surface area with high sensitivity and temporal resolution. We conclude that $P2X_7$ receptor activation increases permeability to mono- and divalent cations and stimulates membrane internalization by a mechanism that is independent of changes in cytosolic Ca^{2+} or cation flux through the ATP-gated channel.

ATP Stimulation of Ionic Current

ATP activates a $P2X_7$ receptor-gated nonselective cation channel in FRTL cells (Kochukov & Ritchie, 2004). This study shows that the channel is also permeable to Ca^{2+} with a P_{Ca}/P_{Cs} of 1.34. This ratio is within the range (1.0–3.9) reported for P_{Ca}/P_{Cs} or P_{Ca}/P_{Na} of other endogenous or heterologously expressed P2X receptors (Evans et al., 1996; Virginio et al., 1998; Liu & Adams, 2001; Bo et al., 2003;). A high concentration of Ca^{2+} (100 mM), however, completely inhibited current activation. This is most likely due to Ca^{2+} chelation of ATP^{4-}, the active agonist for the $P2X_7$ receptor (North, 2002).

The current activated by a submaximal concentration of ATP grew with prolonged or repeated activation of the receptor. At very high concentrations of ATP, the rate of growth was faster, there was slow current decay, and occasionally incomplete deactivation. The ion selectivity did not change dur-

ing the period of current growth, and even during prolonged or repeated activation by 500 μM ATP, P_{NMDG}/P_{CS} remained low (0.11). Low permeability to NMDG is consistent with activation of the $P2X_7$ receptor-gated channel (P_{NMDG}/P_{Na} = 0.03–0.1) (Virginio et al., 1999), but not the slowly activating pore state (P_{NMDG}/P_{Na} = 0.4–0.7) that often follows $P2X_7$ channel gating (Khakh et al., 2001). Absence of pore development was also indicated in previous fluorescence studies on FRTL in which ATP failed to induce permeability to the organic cation YO-PRO-1 (Kochukov & Ritchie, 2004). $P2X_7$ receptor current growth without pore development has been observed by others and could be due to a slowly developing, slowly reversible, increase in potency of ATP (Hibell et al., 2001) or to cytoskeleton-dependent assembly into functional channels (Li et al., 2003). A low-affinity ATP-gated current with a similar priming action of ATP is also present in airway ciliated epithelial cells (Korngreen et al., 1998), although the P2X subtype in those cells is not known.

ATP Stimulation of Decrease in Cell Surface Area

Under standard whole-cell patch-recording conditions, there were no large spontaneous changes in C_m, suggesting that endo- and exocytotic activity were in steady state. Here we show that extracellular ATP induced a slow exponential (τ = 2.7 min) decline in C_m to a plateau level equivalent to loss of ~8% of the cell surface area. It is worthy to note, however, that when 5 mM ATP and 10 μM GTP were included in the pipette solution, extracellular ATP caused a small (3%) net increase in surface area. The increase could be due to inhibition of membrane internalization. If internalization is inhibited, it is likely to be due to the ATP, rather than GTP, since our results with 2 mM GDPβS (described later) indicate that GTP supports internalization. An alternative interpretation is that the nucleotides (mainly ATP) are needed for stimulation of exocytosis (Parsons, et al., 1995; Heidelberger, et al., 2002). In this condition, we presume that both exocytosis and membrane removal are stimulated, but with overall greater addition of membrane. Exocytosis may have a larger energy requirement that is not well supported when cytosolic nucleotides diffuse into the patch electrode. In this study, we used nucleotide-free pipette solution in order to characterize the decrease in cell surface area, although we cannot exclude the possibility that some ATP stimulation of exocytosis is still occurring.

BzATP, an agonist of most P2X receptors, also induced a decrease in C_m. External UTP, a potent agonist of most P2Y receptors but a poor agonist of P2X receptors (Sak & Webb, 2002), had no effect. The P1 adenosine receptor agonist R-PIA was also without effect. The responses to 500 μM ATP were blocked by 100 μM PPADS, 50 μM Cu^{2+} and 200 μM oxoATP, antagonists that are known to be effective at $P2X_7$ receptors. The ATP-induced decrease in C_m shows the same pharmacological specificity as the ATP-gated current and ATP stimulation of FM1-43 internalization in FRTL (Kochukov & Ritchie, 2004) that were previously shown to be mediated by a $P2X_7$ receptor.

In human THP-1 monocytes and HEK cells heterologously expressing $P2X_7$ receptors, receptor activation induces pronounced morphological changes that include blebbing and microvesicular shedding of the plasma membrane into the extracellular medium (MacKenzie et al., 2001). The membrane shedding, like the effect of ATP in FRTL cells, was correlated with a slow (τ = 0.7 min) irreversible decrease in C_m. However, we believe that in FRTL cells the decrease in C_m represents a fundamentally different process. Plasma membrane shedding was entirely dependent on extracellular Ca^{2+}, while in FRTL, the decrease in C_m occurred independently of Ca^{2+} influx or internal Ca^{2+}. In addition, our previous confocal imaging studies with FM1-43 revealed pronounced membrane internalization upon activation of $P2X_7$ receptors (Kochukov & Ritchie, 2004) and no evidence of externalization of membrane fluorescence. Hence, the ATP (500 μM)-induced decrease in C_m largely reflects stimulation of membrane internalization. In comparison to the 8% ATP-induced decrease in cell surface area, the same concentration of ATP stimulated a 27-fold increase in FM1-43-labeled membrane internalization over a similar time period. The unexpectedly high extent of dye internalization is likely explained by the effect of lipid composition on FM1-43 fluorescence intensity (Pappone & Lee, 1996; Zweifach, 2000; Fomina et al., 2003). However, it should also be noted that C_m measurements underestimate the true extent of internalization whenever there is concommitant stimulation of exocytosis and loss of diffusible cytosolic constituents or the contents of the patch pipette solution may additionally influence the electrically recorded response.

The mechanism by which ATP induces membrane internalization is not clear. ATP activation of current preceded the decrease in C_m by ~80 s, raising the possibility that the increase in cation permeability was the trigger for membrane internalization. However, the capacitance response, like ATP stimulation of FM1-43 internalization (Kochukov & Ritchie, 2004), was not dependent on Na^+ or Ca^{2+} influx through the ATP-gated channel. Effects of ATP also persisted upon removal of external Cl^-. Cl^- does not permeate the channel but greatly decreases the potency of ATP activation of $P2X_7$ receptors (Michel et al., 1999). Because heterologously expressed and native $P2X_7$ receptors appear as a strongly bound multimeric complex with numerous other proteins (Kim et al., 2001), the $P2X_7$ receptor could activate

membrane internalization through its interaction with associated proteins (Kochukov & Ritchie, 2004).

ATP stimulation of internalization was readily seen without addition of GTP to the pipette solution; however, including GDPβS (2 mM) in the pipette solution prevented the ATP-induced decrease in C_m. The inhibition by GDPβS was likely due to competition with endogenous GTP that did not completely wash out of the cell during the recording session. It is important to note that GDPβS did not affect the simultaneously monitored ATP-induced changes in G_m, confirming our previous report that ATP activation of current is not G-protein-coupled (Kochukov & Ritchie, 2004). The results suggest that GTP and/or small G-proteins may be involved in mediation of membrane internalization. Small G-proteins, particularly in the rho family of GTPases, are known to regulate membrane trafficking (Lamaze et al., 2001; Schlunck et al., 2004). In addition, the membrane excision step of many different forms of membrane internalization, including phagocytosis (Lamaze et al., 2001; Schafer, 2002; Di et al., 2003), is dependent on the GTPase activity of proteins in the dynamin family (Artalejo et al., 1995; Sever, Damke, & Schmid, 2000). Endocytosis via dynamin-dependent clathrin-coated pits seems to be excluded, however, as the clathrin pathway requires intracellular K^+ (Zuhorn, Kalicharan, & Hoekstra, 2002) and is not supported by patch clamp conditions in which the pipette solution contains Cs^+ as a replacement for K^+ (Artalejo, Elhamdani, & Palfrey, 2002).

Implications

The physiological function of ATP-stimulated membrane internalization is unknown. It is unlikely to reflect $P2X_7$ receptor internalization (Bobanovic, Royle, & Murrell-Lagnado, 2002), as the ionic current activated by 500 μM ATP shows little desensitization during prolonged activation. The high concentrations of ATP that are typically required for activation of $P2X_7$ receptors in physiological salt solutions are mainly encountered upon leakage of cytosolic ATP from membrane-damaged cells. In macrophages, lymphocytes, and other immune cells, $P2X_7$ receptor activation causes pronounced increases in plasma membrane trafficking (MacKenzie et al., 2001; Monleon et al., 2001), events that are important for release of inflammatory mediators, antigen presentation, interaction with phagocytic cells and apoptosis (Coutinho-Silva et al., 1999; Monleon et al., 2001; MacKenzie et al., 2001; Greig et al., 2003). It will be interesting to determine whether the $P2X_7$ receptor induces apoptosis in thyrocytes or if the receptor plays a pathological role in autoimmune diseases such as Hashimoto's thyroiditis where thyrocyte apoptosis is high (Giordano et al., 2001).

We thank Dr. Simon Lewis for transformation of the GHK equation into Equation (1). This work was supported by a Sealy Research Development Grant from the John Sealy Memorial Endowment Fund.

References

Ambesi-Impiombato, F.S., Parks, L.A.M., Coon, H.G 1980. Culture of hormone-dependent functional epithelial cells from rat thyroids. *Proc. Natl. Acad. Sci. USA* **77:**3455–3459

Artalejo, C.R., Henley, J.R., McNiven, M.A., Palfrey, C.H 1995. Rapid endocytosis coupled to exocytosis in adrenal chromaffin cells involves Ca^{2+}, GTP, and dynamin but not clathrin. *Proc. Natl. Acad. Sci. USA* **92:**8328–8332

Artalejo, C.R., Elhamdani, A., Palfrey, H.C 2002. Sustained stimulation shifts the mechanism of endocytosis from dynamin-1-dependent rapid endocytosis to clathrin- and dynamin-2-mediated slow endocytosis in chromaffin cells. *PNAS* **99:**6358–6363

Bo, X., Jiang, L.H., Wilson, H.L., Kim, M., Burnstock, G., Surprenant, A., North, R.A 2003. Pharmacological and biophysical properties of the human $P2X_5$ receptor. *Mol. Pharmacol* **63:**1407–1416

Bobanovic, L.K., Royle, S.J., Murrell-Lagnado, R.D 2002. P2X Receptor trafficking in neurons is subunit specific. *J. Neurosci.* **22:**4814–4824

Bourke, J., Abel, K., Huxham, G., Cooper, V., Manley, S 2001. UTP preferring P2 receptor mediates inhibition of sodium transport in porcine thyroid epithelial cells. *Br. J. Pharmacol.* **127:**1787–1792

Bradford, M.D., Soltoff, S.P 2002. $P2X_7$ receptors activate protein kinase D and p42/p44 mitogen-activated protein kinase (MAPK) downstream of protein kinase C. *Biochem. J.* **366:**745–755

Butler, J.N. 1968. The thermodynamic activity of calcium ion in sodium chloride-calcium chloride electrolytes. *Biophys. J.* **8:**1426–1433

Cerbo, A.D., Corda, D 1999. Signaling pathways involved in thyroid hyperfunction and growth in Graves' Disease. *Biochimie* **81:**415–424

Coutinho-Silva, R, Persechini, P.M., Bisaggio, R.D.C., Perfettini, J.L., Neto, A.C.T.D.S., Kanellopoulos, J.M., Motta-Ly, I, Dautry-Varsat, A., Ojcius, D.M 1999. P2Z/P2X7 receptor-dependent apoptosis of dendritic cells. *Am J. Physiol.* **276:**C1139–C1147

Di, A., Nelson, D.J., Bindokas, V., Brown, M.E., Libunao, F., Palfrey, H.C 2003. Dynamin regulates focal exocytosis in phagocytosing macrophages. *Mol. Biol. Cell.* **14:**2016–2028

Ekokoski, E., Dugué, B., Vainio, M., Vainio, P.J., Tornquist, K 2000. Extracellular ATP-mediated phospholipase A2 activation in rat thyroid FRTL-5 cells: regulation by a Gi/Go protein, Ca^{2+}, and mitogen-activated protein kinase. *J. Cell Physiol.* **183:**155–162

Ekokoski, E., Webb, T.E., Simon, J., Tornquist, K 2001. Mechanisms of P2 receptor-evoked DNA synthesis in thyroid FRTL-5 cells. *J. Cell Physiol* **:187:**166–175

Evans, R.J., Lewis, C., Virginio, C., Lundstrom, K., Buell, G., Surprenant, A., North, R.A 1996. Ionic permeability of, and divalent cation effects on, two ATP-gated cation channels (P2X receptors) expressed in mammalian cells. *J. Physiol* **497:**413–422

Fomina, A.F., Deerinck, T.J., Ellisman, M.H., Cahalan, M.D 2003. Regulation of membrane trafficking and subcellular organization of endocytic compartments revealed with FM1-43 in resting and activated human T cells. *Exp. Cell Res.* **291:**150–166

Giordano, C., Richiusa, P., Bagnasco, M., Pizzolanti, G., Di Blasi, F., Sbriglia, M.S., Mattina, A., Pesce, G., Montagna, P., Capone, F., Misiano, G., Scorsone, A., Pugliese, A., Galluzzo, A 2001. Differential regulation of Fas-mediated apoptosis in both thyrocyte and lymphocyte cellular compartments correlates with opposite phenotypic manifestations of autoimmune thyroid disease. *Thyroid* **11:**233–244

Glass, R., Burnmstock, G 2001. Immunohistochemical identification of cells expressing ATP-gated cation channels (P2X receptors) in the adult rat thyroid. *J. Anat* **198:**569–579

Golstein, P., Abramow, M., Dumont, I.E., Beauwens, R 1992. The iodide channel of the thyroid: a plasma membrane vesicle study. *Am. J. Physiol.* **263:**C590–C597

Greig, A.V.H., Ling, C., Healy, V., Lim, P., Clayton, E., Rustin, M.H.A., McGrouther, D.A., Burnstock, G 2003. Expression of purinergic receptors in non-melanoma skin cancers and their functional roles in A431 cells. *J. Invest. Dermatol.* **121:**315–327

Gu, B.J., Zhang, W.Y., Bendall, LJ, Chessell, IP., Buell, G.N., Wiley, J.S 2000. Expression of P2X7 purinoceptors on human lymphocytes and monocytes: evidence for nonfunctional $P2X_7$ receptors. *Am. J. Physiol.* **279:**C1189–C1197

Hamill, O.P., Marty, A., Neher, E., Sakmann, B., Sigworth, F.J. 1981. Improved patch-clamp techniques for high-resolution current recording from cells and cell-free membrane patches. *Pfluegers Arch.* **391:**85–100

Heidelberger, R., Sterling, P., Mathews, G 2002. Roles of ATP in depletion and replenishment of the releasable pool of synaptic vesicles. *J. Neurophysiol.* **88:**98–106

Hibell, A.D., Thompson, K.M., Simon, J., Xing, M., Humphrey, P.P.A., Michel, A.D 2001. Species and agonist-dependent differences in the deactivation-kinetics of $P2X_7$ receptors. *Naunyn Schmiedebergs Arch. Pharmacol.* **363:**639–648

Khakh, B.S., Bao, X.R., Labarca, C., Lester, H.A. 2001. Neuronal P2X transmitter-gated cation channels change their selectivity in seconds. *Nature Neurosci.* **2:**322–330

Kim, M., Jiang, L.H., Wilson, H.L., North, R.A., Surprenant, A 2001. Proteomic and functional evidence for a $P2X_7$ receptor signalling complex. *EMBO J.* **20:**6347–6358

Kochukov, M.Y., Ritchie, A.K 2004. A $P2X_7$ receptor stimulates plasma membrane trafficking in the FRTL rat thyrocyte cell line. *Am. J. Physiol.* **287:**C992–C1002

Korngreen, A., Ma, W., Priel, Z., Silberberg, S.D 1998. Extracellular ATP directly gates a cation-selective channel in rabbit airway ciliated epithelial cells. *J. Physiol.* **508:**703–720

Lamaze, C., Dujeancourt, A., Baba, T., Lo, C.G., Benmerah, A., Dautry-Varsat, A 2001. Interleukin 2 receptors and detergent-resistant membrane domains define a clathrin-independent endocytic pathway. *Molecular Cell* **7:**661–671

Lejeune, C., Taton, M., Collyn, L., Rocmans, P., Dumont, J.E., Mockel, J 1996. Regulation and metabolic role of phospholipase D activity in human thyroid and cultured dog thyrocytes. *J. Clin. Invest.* **81:**3526–3534

Lewis, C.A. 1979. Ion-concentration dependence of the reversal potential and the single channel conductance of ion channels at the frog neuromuscular junction. *J. Physiol.* **286:**417–445

Li, Q., Luo, X., Zeng, W., Muallem, S 2003. Cell specific behavior of $P2X_7$ receptors in mouse parotid acinar and duct cells. *J. Biol. Chem.* **278:**47554–47561

Lindau, M., Neher, E 1988. Patch-clamp techniques for time-resolved capacitance measurements in single cells. *Pfluegers Arch.* **411:**137–146

Lindenbaum, S., Boyd, G.E 1964. Osmotic and activity coefficients for the symmetrical tetraalkyl ammonium halides in aqueous solution at 25°. *J. Phys. Chem.* **68:**911–917

Liu, D.M., Adams, D.J. 2001. Ionic selectivity of native ATP-activated (P2X) receptor channels in dissociated neurones from rat parasympathetic ganglia. *J. Physiol.* **534:**423–435

MacKenzie, A., Wilson, H.L., Kiss-Toth, E., Dower, S.K., North, R.A., Surprenant, A 2001. Rapid secretion of interleukin-1β by microvesicle shedding. *Immunity* **8:**825–835

Michel, A.D., Chessell, IP., Humphrey, P.P.A. 1999. Ionic effects on human recombinant $P2X_7$ receptor function. *Naunyn Schmiedebergs Arch. Pharmacol* **359:**102–109

Monleon, L, Martinez-Lorenzo, M.J., Monteagudo, L., Lasierra, P., Taules, M., Iturralde, M., Pineiro, A., Larrad, L., Alava, M.A., Naval, J., Anel, A 2001. Differential secretion of Fas ligand- or APO2 ligand/TNF-related apoptosis-inducing ligand-carrying microvesicles during activation-induced death of Human Tells. *J Immunol.* **167:**6736–6744

Nakazawa, K., Hess, P 1993. Block by calcium of ATP-activated channels in pheochromocytoma cells. *J. Gen. Physiol.* **101:**377–392

North, R.A. 2002. Molecular physiology of P2X receptors. *Physiol. Rev.* **82:**1013–1067

Parsons, T.D., Coorssen, J.R., Horstmann, H., Aimers, W 1995. Docked granules, the exocytotic burst, and the need for ATP hydrolysis in endocrine cells. *Neuron* **15:**1085–1096

Pappone, P.A., Lee, S.C. 1996. Purinergic receptor stimulation increases membrane trafficking in brown adipocytes. *J. Gen. Physiol.* **108:**393–404

Robinson, R.A. & Stokes, R.A. 1959 Electrolyte Solutions. The Measurement and Interpretation of Conductance, Chemical Potential and Diffusion in Solutions of Simple Electrolytes. Butterworth & Co.London, UK

Sak, K., Webb, T.E 2002. A retrospective of recombinant P2Y receptor subtypes. *Arch. Biochem. Biophys.* **397:**131–136

Schafer, D.A. 2002. Coupling actin dynamics and membrane dynamics during endocytosis. *Curr. Opin. Cell Biol.* **14:**76–80

Schlunck, G., Damke, H., Kiosses, W.B., Rusk, N., Symons, M.H., Waterman-Storer, C.M., Schmid, S.L., Schwartz, M.A 2004. Modulation of Rac localization and function by dynamin. *Mol. Biol. Cell.* **15:**256–267

Schofl, C., Rossig, L., Potter, E., von zur Muhlen, A., Brabant, G 2002. Extracellular ATP and UTP increase cytosolic free calcium by activating a common P2u-receptor in single human thyrocytes. *Biochem. Biophys. Res. Commun.* **213:**928–934

Sever, S., Damke, H., Schmid, S.L. 2000. Garrotes, springs, ratchets, and whips: putting dynamin models to the test. *Traffic* **1:**385–392

Smallridge, R.C., Gist, I.D. 1994. P2-purinergic stimulation of iodide efflux in FRTL-5 rat thyrocytes involves parallel activation of PLC and PLA2. *Am. J. Physiol.* **267:**E323–E330

Solle, M., Labasi, J., Perregaux, D.G., Stam, E., Petrushova, N., Koller, B.H., Griffiths, R.J., Gabel, C.A 2001. Altered cytokine production in mice lacking P2X7 receptors. *J. Biol. Chem.* **276:**125–132

Virginio, C., MacKenzie, A., North, R.A., Surprenant, A 1999. Kinetics of cell lysis, dye uptake and permeability changes in cells expressing the rat P2X7 receptor. *J. Physiol.* **519:**335–346

Virginio, C., North, R.A., Surprenant, A. 1998. Calcium permeability and block at homomeric and heteromeric P2X2 and P2X3 receptors, and P2X receptors in rat nodose neurones. *J. Physiol.* **510:**27–35

Zuhorn, I.S., Kalicharan, R., Hoekstra, D. 2002. Lipoplex-mediated Transfection of mammalian cells occurs through the cholesterol-dependent clathrin-mediated pathway of endocytosis. *J. Biol Chem.* **277:**18021–18028

Zweifach, A. 2000. FM1-43 reports plasma membrane phospholipid scrambling in T-lymphocytes. *Biochem. J.* **349:**255–260